N89-27791

IEPC 88-126

A TANDEM MIRROR HYBRID PLUME PLASMA PROPULSION FACILITY

88-126

F.R. Chang-Díaz *, T.F.Yang, W. A Krueger, S. Peng,
J. Urbahn, X. Yao, and D. Griffin

M.I.T. Plasma Fusion Center
Cambridge, Massachusetts, 02139

*Astronaut Office
NASA, Lyndon B. Johnson Space Center
Houston, Texas 77058

United States of America

ABSTRACT

A novel concept in electrodeless plasma propulsion, which is also capable of delivering a variable I_{sp}, is presented. The concept involves a three-stage system of plasma injection, heating and subsequent ejection through a magnetic nozzle. The nozzle produces the hybrid plume by the coaxial injection of hypersonic neutral gas. The gas layer, thus formed, protects the material walls from the hot plasma and, through increased collisions, helps detach it from the diverging magnetic field. The physics of this concept is being evaluated numerically through full spatial and temporal simulations; these explore the operating characteristics of such a device over a wide region of parameter space. An experimental facility to study the plasma dynamics in the hybrid plume has also been built. The initial experimental device consists of a tandem mirror operating in an asymmetric mode. The plasma is initially generated by ECRH breakdown of neutral gas and later RF heated to hundreds of electron volts at the Ion Cyclotron Resonance frequency. A latter upgrade of this system will incorporate a cold plasma injector at one end of the machine. Initial experiments involve the full characterization of the operating envelope, as well as extensive measurements of plasma properties at the exhaust. The results of the numerical simulations, as well as the facility itself and its planned upgrades, will be described in detail.

INTRODUCTION

The finite and, most likely, limited availability of electric power for space applications has important implications in electric propulsion. First, the current efforts to achieve high specific impulse cannot be achieved without drastic penalties in thrust. Moreover, even currently projected power levels at high I_{sp} imply severe damage to material surfaces such as electrodes and nozzles.

If the availability of electric power were not limited, then clearly the best approach to electric propulsion is a high I_{sp}. It would not matter that the required rocket power increases as I_{sp}^3, provided, of course, that suitable materials could be found to reliably process and direct this power. Realistically, however, even the most ambitious electric power concepts are unlikely to provide such virtually unlimited power levels, nor are we likely to design an electrode configuration which could withstand them.

One approach that effectively circumvents these two problems is the variable I_{sp} Hybrid Plume Rocket (**Refs. 1, 2**). In this approach, the materials problems are ameliorated by an electrodeless magnetic confinement scheme borrowed from the Tandem Mirror approach to controlled thermonuclear fusion. Additionally, this concept features a specialized two-stage magnetic nozzle with an annular hypersonic coaxial gas injector near the throat. This is shown schematically in **Fig. 1**.

Figure 1

Schematic view of the Hybrid Plume Rocket.

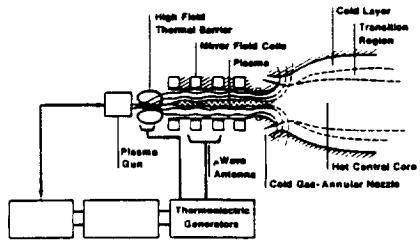

Since the available power is limited, the Hybrid Plume Rocket seeks to continuously optimize the thrust/I_{sp} combination in relation to the vehicle velocity. This continuous, real-time tuning maximizes the equation:

$$\eta = \frac{2\frac{v}{u}}{1+\left(\frac{v}{u}\right)^2} \qquad (1)$$

where η denotes the rocket propulsive efficiency in free space and in the absence of gravitational effects. The quantities v and u denote the vehicle and exhaust velocities respectively. Optimum efficiency occurs when $v = u$.

The vehicle velocity is, of course, frame dependent. The proper frame, in this case, is that where the rocket fuel was loaded. The functional dependence on the velocity ratio is intuitively obvious: if each element of the exhaust flow leaves the rocket at rest, it gives up all of its kinetic energy to the vehicle. High, or low exhaust velocities, with respect to the vehicle, lead to propulsive inefficiency.

In addition to variable I_{sp}, the Hybrid Plume Rocket has two other attractive features. First, the creation of a relatively dense coaxial neutral boundary layer near the nozzle throat provides an effective insulation protecting the material wall from the hot plasma. Second, the presence of the gas enhances the collision rate near the wall providing an effective mechanism for detaching the plasma from the magnetic field.

BASIC EQUATIONS

The basic momentum balance for a rocket in free space and assuming no gravitational effects can be expressed as

$$v' = -\frac{u\,m'}{m} \tag{2}$$

where v' and m' are time derivatives of the vehicle velocity and rocket total mass respectively.

The rocket exhaust power flow can be expressed as

$$P = m'\frac{u^2}{2} \tag{3}$$

and the various rocket masses are related as follows:

$$m = m_o - m_f \tag{4}$$

where m_o is the total mass of rocket and fuel at $t = 0$, and m_f is the total mass of fuel exhausted through the nozzle at time t.

If the assumption that $u \equiv constant$ is made at this point, integration of Eq.2 between the limits of v_o and v (i.e., initial and final velocities), yields the familiar rocket equation:

$$v(t) = v_o + u\,ln\frac{1}{1-\beta t} \tag{5}$$

where β is defined by the equation

$$\beta \equiv \frac{\dot{m}}{m_o} = \frac{m_f}{m_o t} = \frac{\gamma}{t} \tag{6}$$

The mass flow rate $\dot{m}$ is normally considered to be a constant. In Eq.6, the quantity $\gamma \equiv m_f/m_o$ is the mass fraction.

However, if instead the assumption is made that $u \equiv v$, in acordance with the optimum in Eq.1, integration of Eq.2 produces a simple linear result:

$$\frac{v}{v_o} = \frac{m_o}{m} \tag{7}$$

and, in terms of the mass fraction γ

$$v = v_o\left(\frac{1}{1-\gamma}\right) \tag{8}$$

Equation (8) is shown plotted in **Fig. 2** as a function of γ. For comparison, the same velocity ratio profile for a constant I_{sp} chemical rocket, with $u/v_o = .5$, is shown as a dashed curve. One can view this result in two ways: first, for the same mass fraction, the hybrid rocket can achieve significantly greater velocities; and second, for the same terminal velocity, the hybrid plume rocket represents a substantially lower mass fraction and, hence, a substantially greater payload capacity.

Figure 2

Velocity ratio as a function of the fuel mass fraction γ for the Hybrid Plume Rocket (shown by solid curve) and a conventional chemical rocket (shown by the dashed curve) with $u/v_o = .5$.

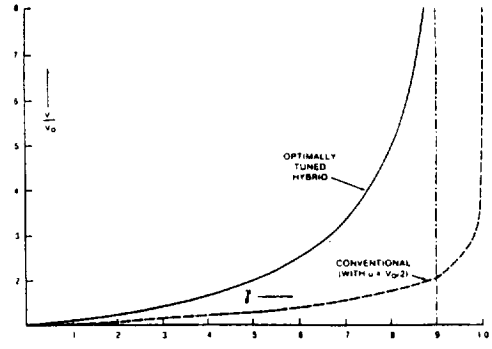

In this regard, it must also be pointed out that a constant, high I_{sp} rocket is also attractive. However, the Hybrid Plume concept has some added advantages over even this latter approach. This will be shown next.

TIME DEPENDENT ROCKET PERFORMANCE

In order to be desirable, the Hybrid Plume Rocket must also have sufficient acceleration. Accordingly, it is important to obtain a relationship for v as a function of time. Such relationship will be derived next.

Using Equations 7 and 3, with $v = u$, one can write:

$$\frac{2P}{\left(v_o m_o\right)^2}dt = \frac{dm}{m^2} \tag{9}$$

Integration of this expression yields:

$$\frac{2Pt}{\left(v_o m_o\right)^2} = -\int_{m_o}^{m}\frac{dm}{m^2} \tag{10}$$

where the negative sign has been introduced to account for the decreasing mass. Integrating each side one obtains

$$\frac{1}{m_o} + \frac{2Pt}{\left(v_o m_o\right)^2} = \frac{1}{m} \tag{11}$$

and solving for m as a function of time gives the time-dependent spacecraft mass:

$$m(t)=\frac{1}{\frac{1}{m_o}+\frac{2Pt}{\left(m_o v_o\right)^2}} \tag{12}$$

From this expression one can calculate the burnup time τ by defining the dry mass of the rocket m_r so that

$$\tau=\left(1-\frac{m_r}{m_o}\right)\frac{v_o^2 m_o^2}{2Pm_r} \tag{13}$$

Equations 7 and 12 can now be combined to obtain velocity as a function of time; the result is:

$$v(t)=v_o+\frac{2Pt}{v_o m_o} \tag{14}$$

Integration of Equation 14 yields the distance χ as a function of time:

$$\chi(t)=v_o t+\frac{Pt^2}{v_o m_o} \tag{15}$$

Note, from Eqs.14 and 15 that an optimally tuned, variable I_{sp} rocket operates at a constant acceleration equal to $2P/v_o m_o$.

Figure 3 shows a comparison of trip times as functions of the total fuel required for the constant I_{sp} rocket and the optimally tuned hybrid. The fixed quantities in this graph are: total payload, total distance and power level.

Figure 3

Trip time as a function of fuel mass for the constant I_{sp} rocket (solid curve) and the optimally tuned, variable I_{sp} concept (solid dot on lower right of graph). The curves were plotted assuming the same mission parameters (shown in upper right) for both rockets.

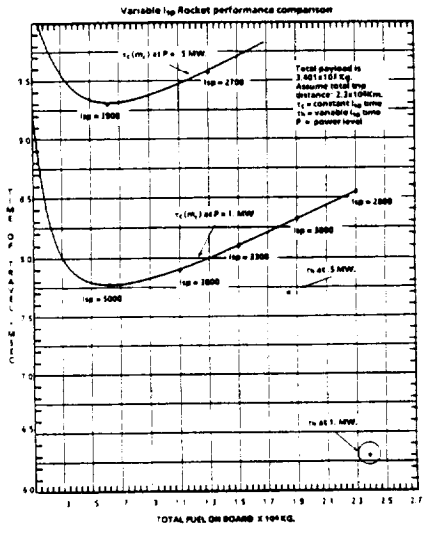

Several issues can be discussed from Fig. 3. First, the constant I_{sp} rocket has an infinite number of solutions yielding a continuous curve. For the case considered, this curve has a minimum at about $m_f = 0.6\times10^4$ Kg and $t = 7.775\times10^6$ sec. The I_{sp} consistent with this minimum is 5.2×10^3 sec. Higher values lead to longer trip times because the thrust is too low; whereas, lower values also result in longer trip times because the vehicle is too "fuel-heavy."

Second, the optimally tuned hybrid yields only one design point. This is a result of the optimization leading to Eq. 6. For the case presented here, the fuel required is about four times higher while the trip time is reduced by about 20%. Similar comparisons can be drawn for other missions, payloads and power levels.

In general, it can be seen that for short missions, the hybrid produces only marginal gains in trip time over the constant high I_{sp} rocket, provided, of course, that the required constant I_{sp} and power level can be reliably produced.

At lower values of constant I_{sp}, for the same power level, the hybrid becomes more attractive. For example, comparison with a constant I_{sp} rocket at, say 3000 sec., shows the hybrid's gain to be a 27% shorter trip time for the same amount of fuel. Moreover, it can be shown that as the total mission distance is increased, the fractional gains in trip time for the hybrid plume become greater.

In short, the Hybrid Plume Rocket reduces to the constant I_{sp} one for short distances and, hence, low Δv. For high Δv and long distances, the Hybrid becomes much more attractive.

NUMERICAL MODELING

The physics of high temperature hydrogenic plasmas, interacting with hypersonic gas jets are not well-understood. Analytical and numerical modeling of these interactions requires the simultaneous, self-consistent solution of particle, momentum and energy transport equations for each particle species. Moreover, the solution approach must have sufficient spatial granularity to resolve small regions of the flow pattern.

In the present problem, the Hybrid Plume concept relies on the stable injection of hypersonic neutral gas, coaxial to a hot plasma column. This plasma column is created and heated to hundreds of ev in the central cell of a Tandem Mirror magnetic confinement system (**Ref. 3**).

Figure 4

Geometric contour of diverging magnetic field lines within the exhaust duct. The figure also shows neutral density contours for a thin gas jet injected at a radial distance of 5 cm from the duct center line.

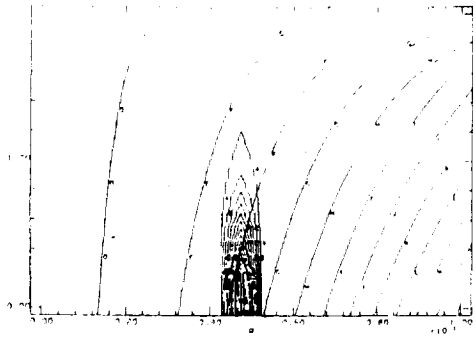

This complex scenario is currently being examined numerically by means of a three-dimensional, time-dependent multifluid code (**Ref. 4**). The present simulation models the flow dynamics, as well as the various particle interactions, such as ionization, recombination and charge exchange, in the presence of an externally applied magnetic field. This code is not yet fully operational, but some of its salient features are shown on **Figs. 4, 5 and 6.**

Figure 5

Plasma density contours with neutral gas injection.

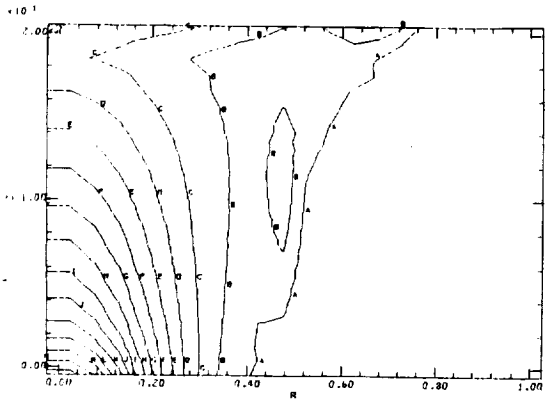

Fig. 4 shows the injection of a thin neutral gas jet at a radial distance of 5 cm from the duct center line. The figure also shows the diverging magnetic field lines in which the plasma is immersed. **Fig. 5** shows the effect of hot plasma injection into the configuration of **Fig. 4** and the formation of a dense plasma layer (contour B). Finally, **Fig. 6** shows the plasma flow with no gas present.

Figure 6

Plasma density contours with no gas injection.

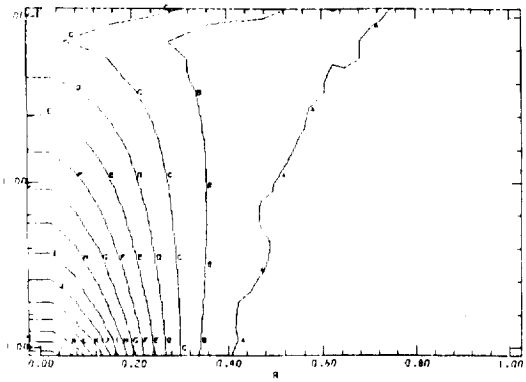

This numerical code continues to be refined and will be used as a tool to extrapolate the results of the experimental program. This latter one is our most recent undertaking and will be discussed in detail next.

EXPERIMENTAL STUDIES

Initial experimental characterization of the physics and engineering of hybrid plumes has recently been undertaken in our laboratory. To this end, a plasma facility in the form of a small tandem mirror has been built and recently tested successfully.

Figure 7

Trimetric view of the tandem mirror machine.

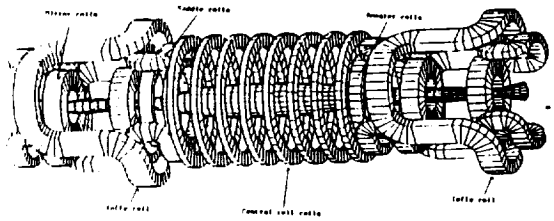

The tandem mirror (**Fig. 7**) is a versatile, open ended, linear plasma generator capable of operating in a variety of experimental regimes. The device consists of two magnetic mirrors, called "plugs" or "anchors," joined together by a long solenoidal section called the "central cell." While the plasma in this device spans the entire length of the machine, its pressure is higher in the plugs than in the central cell.

In the tandem mirror, the central plasma is not only magnetically confined, but a certain low energy class of particles is electrostatically trapped as well. This latter confinement feature is created by a positive ambipolar potential, intentionally maintained between the plugs and the central cell through differential heating.

In contrast to its use for fusion, a tandem mirror, operating as a thruster, implies that one of the plugs must be "weaker" than the other, thus establishing a preferred flow direction. The demonstration of this asymmetric mode of operation is one of the main objectives of this experiment.

In this system, plasma parameters like density, temperature and particle confinement time can be selectively controlled by a variety of means (**Refs. 5 and 6**). For example, particle density can be regulated magnetically by constricting the magnetic field at the plugs, or electrostatically by increasing the positive ambipolar potential. Moreover, the longer particle confinement times of the tandem, relative to the simple mirror, imply the potential for higher plasma densities. This fact will, undoubtedly, result in an expanded operational envelope.

Figure 8

Schematic view of the experimental device for variable I_{sp} plasma propulsion studies.

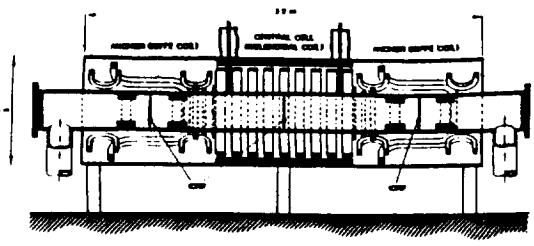

The present experimental configuration is shown schematically in Figs. 8 and 9. It consists of 8 central cell coils, 8 mirror coils and four booster coils. The two sets of Ioffe and Saddle coils shown in Fig. 7 have not been added yet and will not be required for plasma MHD stability until the system goes to high temperature operation.

As shown in Fig. 8, the machine measures 3 m in length by .75 m in diameter. The vaccum chamber is a cylindrical assembly composed of nine stainless steel sections. It has a total of 24 access ports for plasma diagnostics. Two turbomolecular pumps and two mechanical forepumps are sufficient to create a tight vacuum at 10^{-8} Torr. within a few hours. The main system parameters are listed in Table 1.

Table 1

System parameters

Overall length	3.2 m
Central cell length	1.15 m
Central cell radius	0.36 m
Central cell field (B_c)	1.2 kG
Maximum field (B_{max})	15.0 kG
Minimum field in the plug (B_{min})	6.3 kG
Plasma density (variable)	10^{13} cm^{-3}
Plasma temperature	.01 - 1.0 kev
Magnet power dissipation:	
• At room temperature	523. kW
• At liquid nitrogen temp.	80. kW
• Superconducting	0.0 kW
Plasma heating power:	
• ECRH	2.0 kW
• ICRH	100.0 kW

Figure 9

Trimetric view of experimental device and major components.

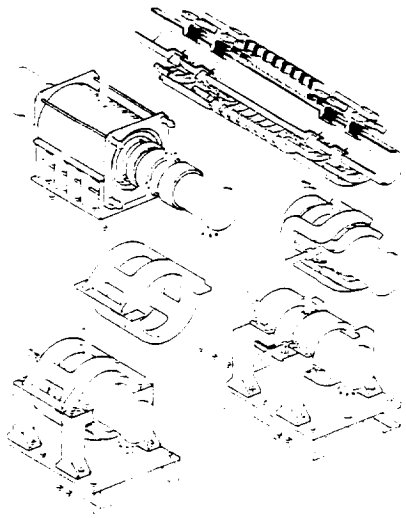

The 8 central cell coils are each enclosed in a liquid nitrogen case. The mirror coils also have their liquid nitrogen casing as well as a vacuum jacket for additional thermal insulation. This latter set of coils are built directly onto the chamber structure. A mechanical pumping line, connected to a common manifold, provides the vacuum for the mirror coils. The booster coils dissipate low power and require no active cooling. Internally, each coil is separated from its casing by a special spring of our own invention. Each of these springs must be able to resist the thermal and magnetic stresses while minimizing thermal conduction. Moreover, the springs must be electrically isolated from the coil wingings.

Plasma generation

The plasma is created through a variety of mechanisms depending on the particular experimental requirement. 1.) A glow discharge probe has been installed to produce a low temperature plasma at gas pressures of the order of 30 mTorr. This is mainly used for discharge-cleaning the inner walls of the chamber. 2.) An Electron Cyclotron Resonance Heating (ECRH) antenna, operating at a frequency of 2.4 GHz, has also been installed to generate low temperature plasma discharges at pressures of a few mTorr. This system is used to preionize the gas before RF power is injected. The RF system will be in the form of a 100 kW Ion Cyclotron Resonance Heating (ICRH) radio frequency power transmitter. This system is currently under construction.

Plasma diagnostics

Several types of plasma diagnostics are envisioned. However, during the initial phases of the experiment the plasma bulk pressure will be measured by a set of diamagnetic loops in both the plugs and the central cell. An array of Langmuir probes will be used to measure density and temperature at the plasma edge. A surplus laser fluorescense system has been obtained and will be set up to measure neutral density. A retarding potential particle energy analyzer will be implemented at a later time to directly measure the plasma properties at the exhaust. The average plasma density will be measured by microwave interferometry.

Recently, our team has also entered into cooperation with the T.V. Laboratory of the NASA Johnson Space Center to incorporate some of the Space Shuttle low-light-level and U.V. equipment to view the plasma discharge in real time. More advanced instrumentation will be added as it becomes available.

Present status

The final assembly of the basic device was completed in July of 1988. Testing has proceeded at 10% of rated power and field strength. This mode has allowed steady state operation without liquid nitrogen and enabled us to map and fine-tune the magnetic field profile.

While we plan to eventually automate, the present operation is entirely manual. The first plasma discharge was achieved in mid August.

Ongoing work

Presently, the machine is operating at low power levels. The liquid nitrogen system will be activated and the vacuum line for the mirror coils is being installed. Also being installed are: a laser fluorescence diagnostic system to measure neutral density, the Langmuir probes, diamagnetic loops and associated electronics and the microwave interferometer.

Figure 10

Block diagram of the ICRH transmitter system.

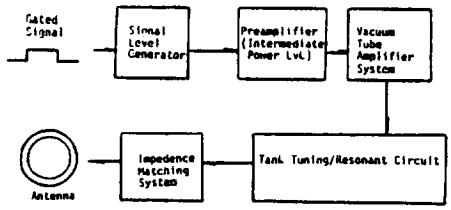

The ICRH system is now designed and under construction. A block diagram of this design is shown in **Fig. 10**. The RF antennae, **Fig. 11**, are also designed and under construction.

Figure 11

Schematic representation of the ICRH antenna.

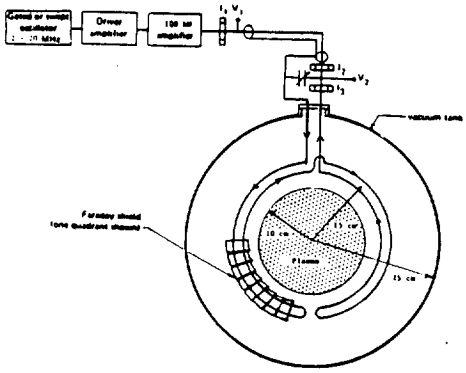

The tasks for the next few months will involve a full characterization of the plasma properties and the operating envelope of the machine. This will set the stage for a large array of experiments designed to test the variable I_{sp} capabilities of this device as well as in-situ measurements of the exhaust plasma.

CONCLUSION

In addition to its variable I_{sp}, the Hybrid Plume Rocket is capable of effectively insulating the nozzle walls from the hot plasma. This feature is obtained by the presence of a cold, hypersonic outer gas envelope between the wall and the plasma core. Moreover, the presence of the gas also helps detach the plasma flow from the diverging magnetic field.

The continuous optimal tuning of thrust and I_{sp} produces a linear rocket equation and implies operation at constant acceleration. The utilization of variable I_{sp} for short, low Δv missions produces only marginal advantages; however, it produces substantial gains for long, high Δv missions.

The Hybrid Plume concept has been modeled with a full time-dependent, multifluid code. More recently, a small tandem mirror device has been built as the first stage of an experimental demonstration of the Hybrid Plume. The device was completed in July of 1988 and initial low temperature plasma discharges have already been produced. A full complement of plasma experiments and full power operation are expected in the upcoming months.

ACKNOWLEDGEMENT

This work was supported by the Office of Scientific Research, U.S. Air Force, and the U.S. National Aeronautics and Space Administration.

REFERENCES

1. F. R. Chang; The Hybrid Plume Rocket; NASA/ Johnson Space Center, Internal report, January 1982.

2. T. F. Yang, et. al; A Tandem Mirror Plasma Source for a Hybrid Plume Plasma Propulsion Concept; MIT Plasma Fusion Center, Cambridge, Mass.; AIAA/DBLR/JSASS Intl. Electric Prop. Conf., Alexandria, Va., U.S.A., September 1985.

3. D. E. Baldwin and B. G. Logan; TMX Major Project Proposal; Lawrence Livermore National Laboratory Report: LL-PROP-148 (1977).

4. F. R. Chang, W. A. Krueger and T. F. Yang; Numerical Modeling of the Hybrid Plume Plasma Rocket; MIT Plasma Fusion Center, Cambridge, Mass., U.S.A.; AIAA/DBLR/JSASS, Intl. Electric Prop. Conf.; paper: AIAA 85-2058, Alexandria, Va., U.S.A., September 1985.

5. W. C. Turner, et. al.; Recent Experimental Progress in the TMX-U Thermal Barrier Tandem Mirror Experiment; Lawrence Livermore National Laboratory Report: UCRL-90879, preprint 1984.

6. R. Bruen, et. al.; Initial Results From the Tandem Mirror Phaedrus; IAEA Tenth Conf. on Plasma Physics and Controlled Nuclear Fusion Res.; paper: IAEA-CN-44/C-II-5, 359, Vienna, 1985.